www.csiro.au

IMOS Integrated Marine Observing System

Ocean Colour Sub-Facility

Ocean Colour Validation Report

2016-17

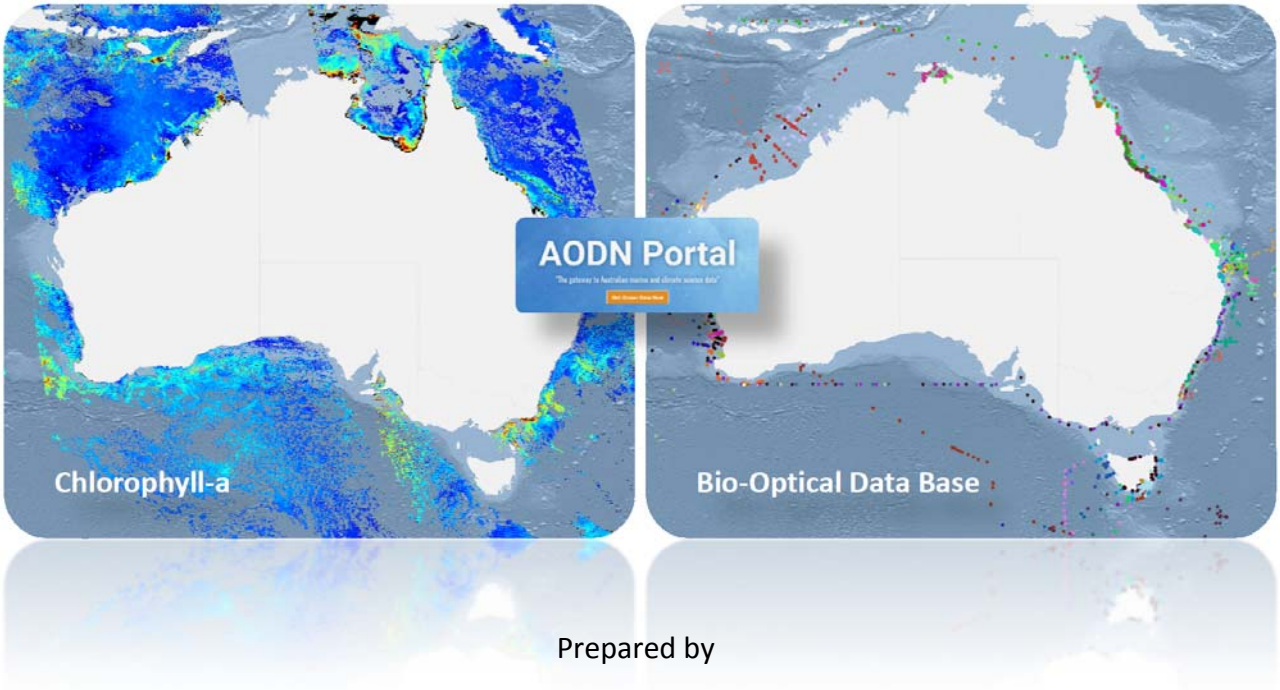

Prepared by

Thomas Schroeder, Jenny Lovell, Edward King, Lesley Clementson, Roger Scott

CSIRO Oceans and Atmosphere

June 2017

Citation

Schroeder T., Lovell J., King E., Clementson L., and Scott R., (2017), IMOS Ocean Colour Validation Report 2016-17, Report to the Integrated Marine Observing System (IMOS), CSIRO Oceans and Atmosphere, 23 pp.

Copyright and disclaimer

Important disclaimer

Cover Images

Snapshots of the Australian Ocean Data Network (AODN) Portal displaying two subsequent MODIS-Aqua orbits of GSM chlorophyll-a around Australia (left) and the corresponding spatial distribution of IMOS Bio-Optical Data Base measurements.

Contents

Figures

Tables

1 Introduction

In this second IMOS Ocean Colour validation report we provide an update on the accuracy assessment of four different chlorophyll-a (chl-a) products, namely *OC3* (O'Reilly et al., 2000), *OCI* (Hu et al, 2012, Wang and Son, 2016), *GSM* (Maritorena et al., 2002) and *Carder* (Carder et al., 1999, 2003), that are computed and distributed by the IMOS Ocean Colour Sub-Facility.

Product validation is achieved through match-up analysis, comparing the satellite derived chl-a products to *in situ* observed chl-a measurements close to the satellite overpasses within the wider Australasian marine region ([10°N,80°E]-[60°S,180°E]).

In situ data for validation however are not available in every region and some marine areas around Australia (e.g. the Great Australian Bight, Tasman Sea or the Gulf of Carpentaria) are sparsely or not at all covered by ground observations. To enable product validation in these under-sampled regions, the Ocean Colour Sub-Facility has adopted a validation approach that is based on a classification of Optical Water Types (OWT, Moore et. al 2009). This approach assumes that the match-up results obtained for a given water type can be used to estimate the accuracy of a specific Ocean Colour product in the absence of ground observations with the help of a corresponding satellite-derived water type map. Water type maps are produced by IMOS as a separate ocean colour product to guide this accuracy interpretation.

The *in situ* chl-a data for this comparison were extracted from the IMOS Bio-optical Data Base, which collates in-situ discrete physical, bio-geochemical, and optical data collected by the by the Australian bio-optical community from 1997 to date.

Significant additions to the Bio-optical Data Base were achieved during the 2016-17 reporting period and specifically the large data sets provided by the Australian Institute of Marine Science (AIMS) and James Cook University (JCU) for the Great Barrier Reef region, led to a significant increase in the number of valid chl-a match-ups for both VIIRS and MODIS Aqua compared to the previous reporting period.

The MODIS match-up data for the *OC3* algorithm for example, with a time difference (ΔT) of ±2 hours to the *in situ* data, more than doubled and increased from N=413 in 2015-16 to N=1,085 for this reporting period. More importantly the VIIRS match-ups increased significantly now allowing a split into Optical Water Types (OWT), which was not possible in 2015-16 when only N=32 match-up were reported. For this report match-ups increased to N=836 for the *OC3* algorithm at ΔT=±24 h and N=510 at ΔT=±2 h.

The IMOS baseline processing system for MODIS and VIIRS remains unchanged since the last reporting period. It is based on SeaDAS version 7.3.1 and included regular updates to calibration files and Look-up-Tables released by NASA.

A detailed summary of the IMOS satellite data processing system and a description of the validation methodology are provided in the 2015-16 report (Schroeder et al., 2016).

This report provides a brief summary on the 2016-17 water type-based chl-a validation results for the Australasian marine region.

2 Results and discussion

The accuracy of satellite-derived chl-a products generated and distributed by the IMOS Ocean Colour Sub-Facility were evaluated using *in situ* chl-a observations collated by the IMOS Bio-optical Data Base activity. The comparison was performed for the full mission time series of the MODIS-Aqua and the VIIRS Suomi-NPP Ocean Colour sensors covering the Australasian marine region.

The range of *in situ* measured chl-a extracted from the Bio-optical Data Base and used in the match-up analysis covered three orders in magnitude [0.01-10] mg m^{-3}. Due to the significant increase in available measurements for validation, statistics became more robust for this reporting period, especially when splitting into water types. However, measurements for OWT 5, representing highly absorbing CDOM-rich waters, remain under-sampled and were not available in sufficient number to validate algorithms for either MODIS or VIIRS.

As already noted for the last reporting period large observational gaps in *in situ* chl-a still exist for the Tasman Sea, Gulf of Carpentaria and the Great Australian Bight.

The water type-combined match-up analysis for MODIS-Aqua showed that all algorithms overestimated chl-a compared to the *in situ* measurements indicated by their positive bias. At ΔT=±2 h and for the OWT-combined match-ups the smallest bias of 0.07 mg m^{-3} was observed with the *Carder* algorithm, while OCI showed the largest bias of 0.37 mg m^{-3}. When match-ups were split into OWTs only Carder showed a negative bias underestimating chl-a for OWTs 1-3 within the same ΔT. In terms of percentage error *Carder* performed best across all OWTs on MODIS except for OWT 6. In open ocean waters *OCI* showed a slight improvement compared to *OC3* reducing the percentage error from 97% to 86% for OWT 1. With 206% error *GSM* performed worst on MODIS for the open ocean waters represented by OWT 1. The retrieval performance was generally low for all algorithms applied to MODIS in coastal waters, e.g. across OWTs 4-8 showing errors of up to 590%.

The application of *OC3* and *GSM* to VIIRS showed overall a decreased performance compared to their application to MODIS, with OWT-combined *OC3* retrieval errors of 308% for VIIRS compared to 273% with MODIS, and *GSM* errors of 530% for VIIRS compared to 230% with MODIS at ΔT=±2 h. The correlation between *in situ* and VIIRS *GSM* chl-a is extremely low (R^2<0.08) due to the significant overestimation at lower concentration levels <1 mg m^{-3} (Fig 5). Average *OC3* retrieval errors for OWT 1-3 were 86% while *GSM* errors exceeded 1,200%. While the water type-combined number of match-up for VIIRS were sufficient for this analysis (N=510 OC3, N=416 GSM, ΔT=±2 h), their split into water types remain sparse for OWT 1 with N=9 (open ocean waters), and OWT 4 with N=8 and OWT 5 with N=1 (high CDOM waters). Correlations between *in situ* and VIIRS *GSM* derived chl-a are low across all water types. Better correlations are achieved with VIIRS *OC3* especially for water types 1, 6, 7, and 8.

The overall poor results for coastal waters highlight the need for more accurate ocean colour algorithms.

This water-type based validation approach could be extended to other satellite products with a sufficient number of matching ground observations.

Match-up statistics of the 2015-16 report are superseded by the results provided with this report.

Recommended product use

- **For VIIRS:** Use *OC3* over *GSM* in marine regions with water types 1-4. Chl-a errors in regions associated with water types 6-8 exceed 200% for both algorithms applied to VIIRS. Data in these regions should be used with care.
- **For MODIS Aqua:** Use *Carder* in marine regions with water types 1-4. Chl-a errors in regions associated with water type 4 however exceed 400%. Also use *Carder* in regions with water types 7 and 8 and *GSM* for water type 6 applied to MODIS.

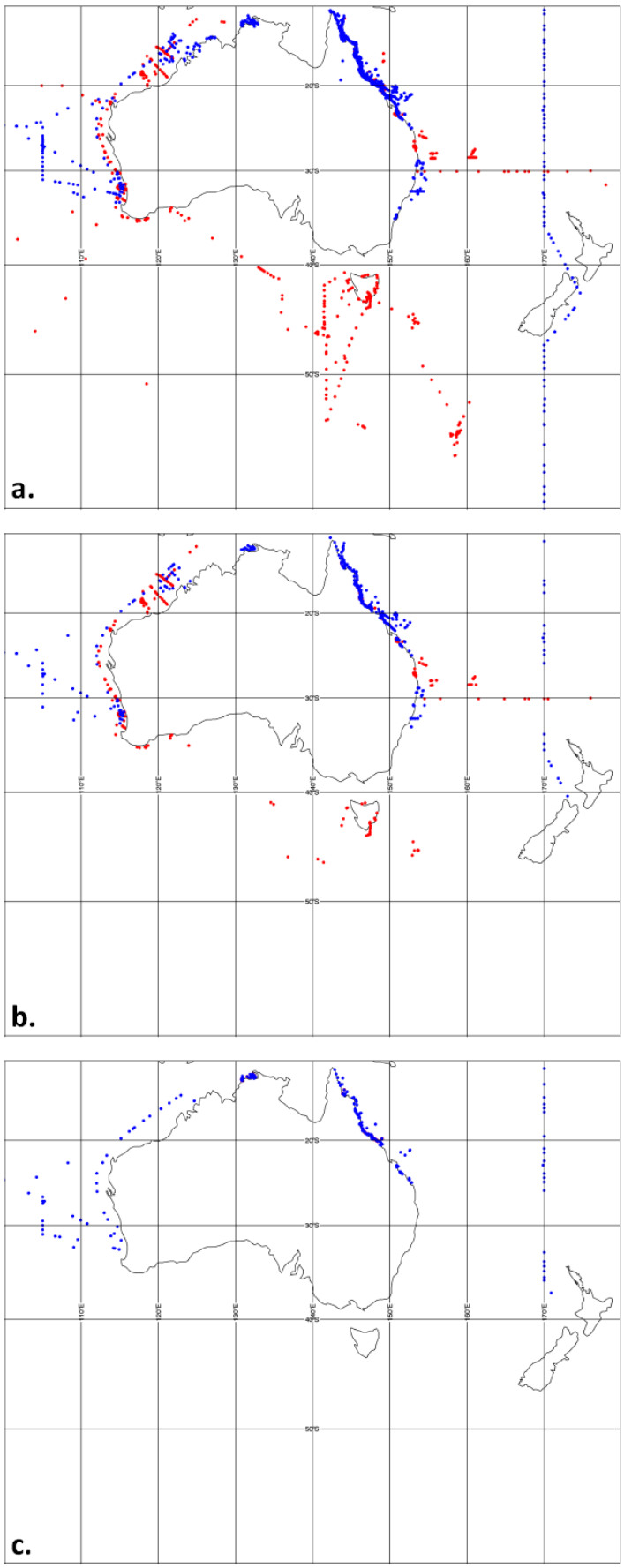

Figure 1 (a) Location of all *in situ* chl-a measurements, red dots included in 2015-16 report, blue dots, new data added in this report. (b) Location of in situ chl-a measurements matched with MODIS observations. (c) Location of in situ chl-a measurements matched with VIIRS observations. Maximum time difference ΔT between in situ and satellite data for this plot is ±24 h.

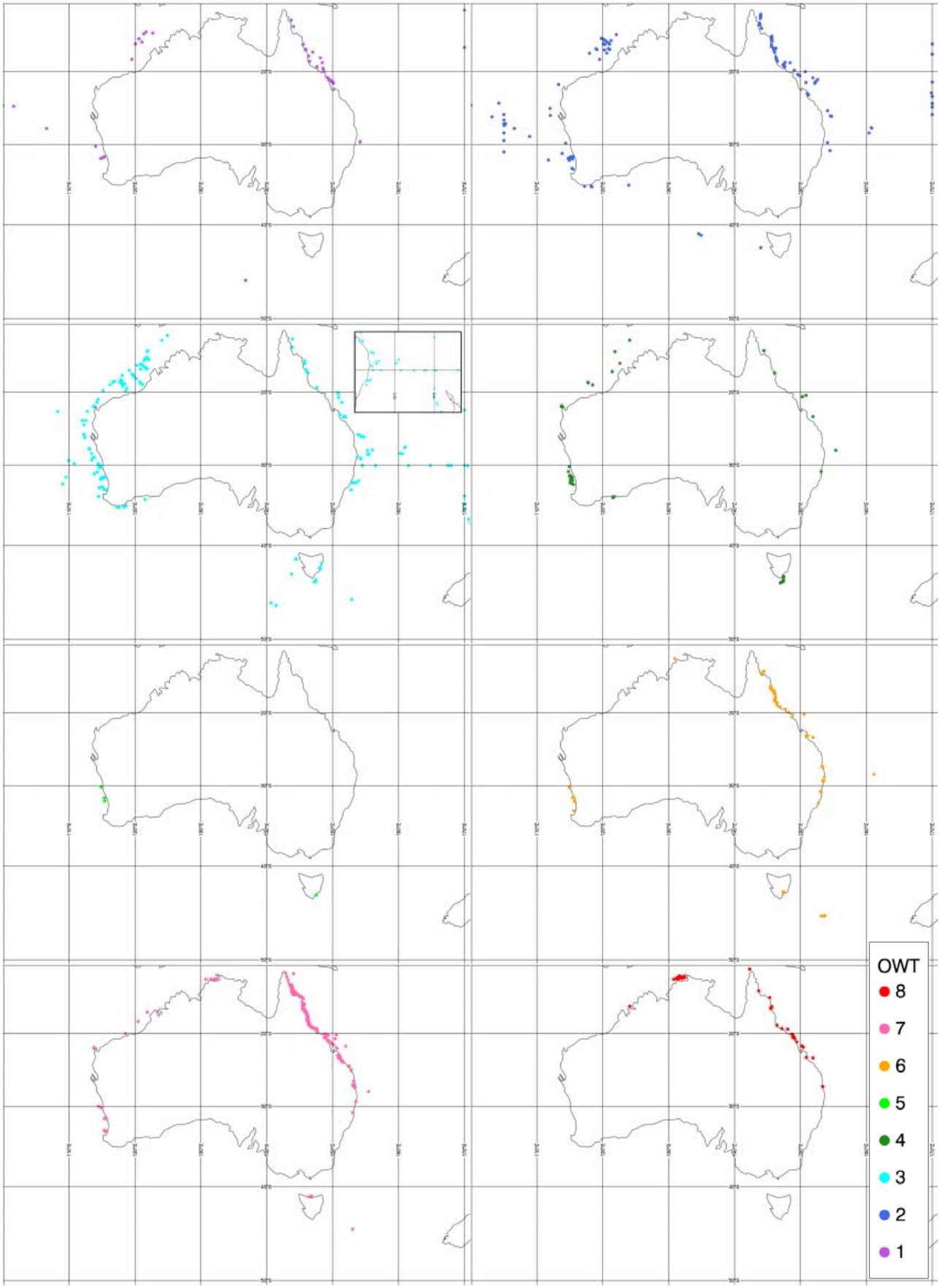

Figure 2 Spatial distribution of MODIS-Aqua chl-a match-up data (Fig 8b) classified by OWT (ΔT=±24 h).

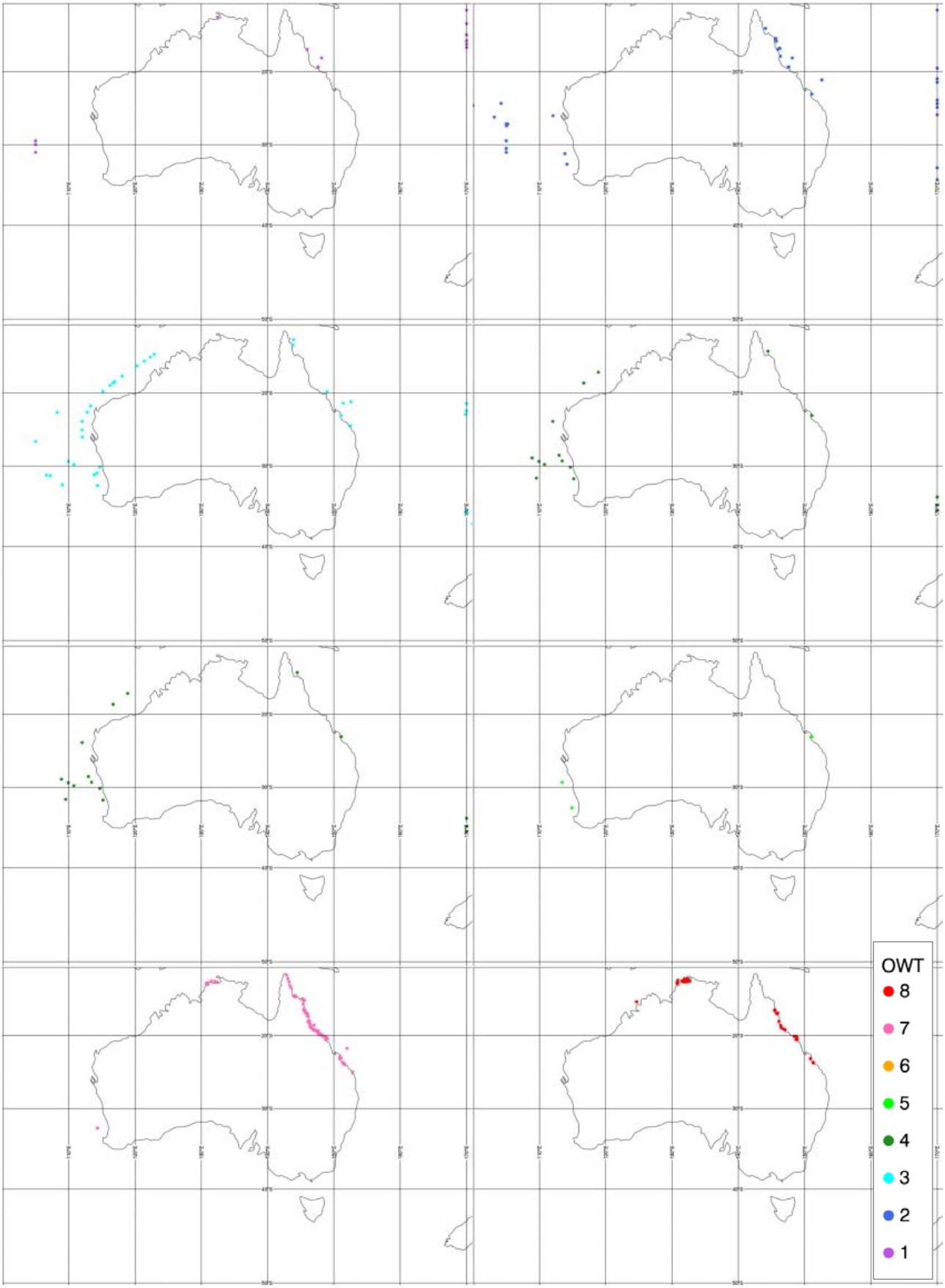

Figure 3 Spatial distribution of VIIRS chl-a match-up data classified by OWT (ΔT=±24 h).

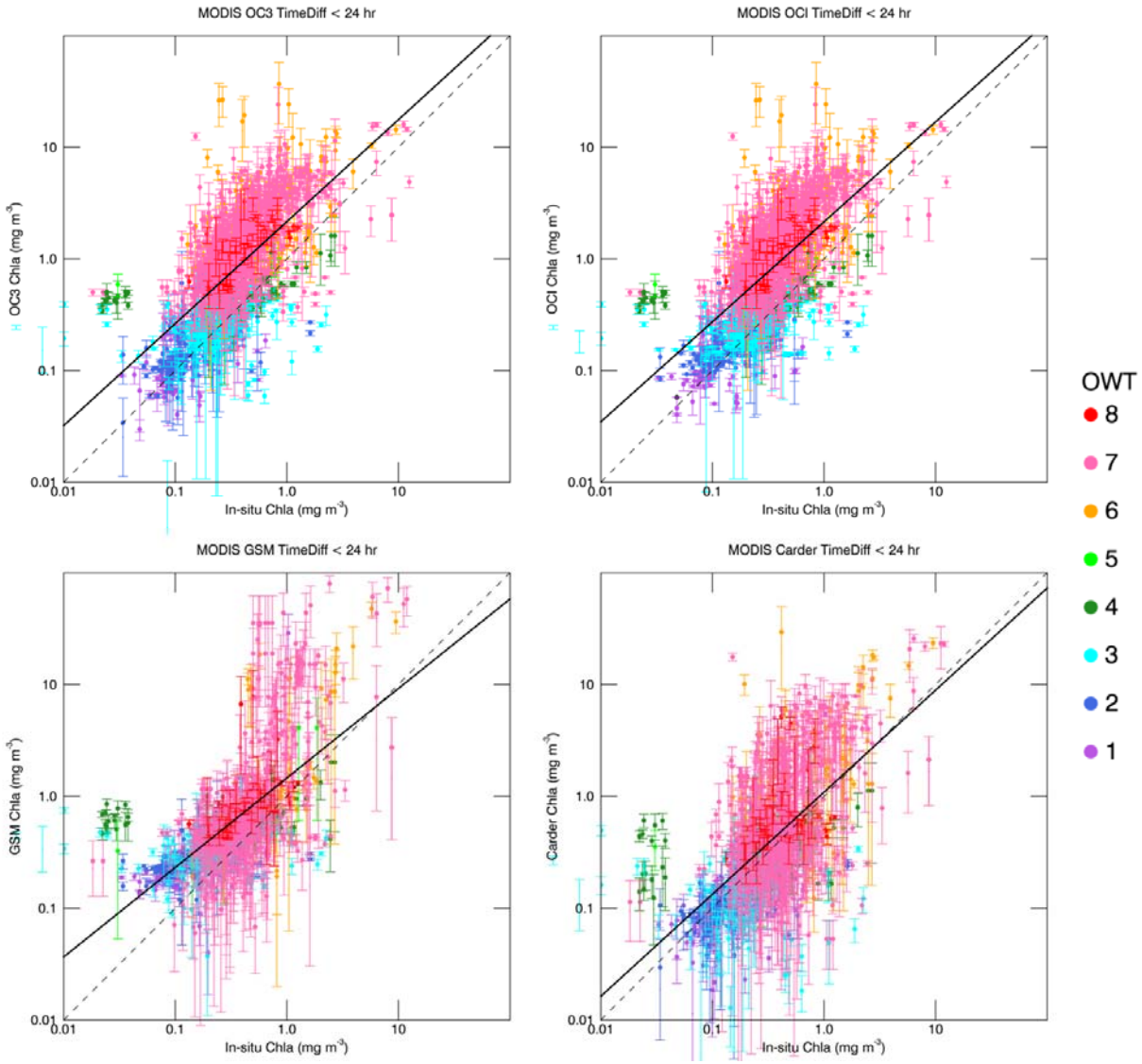

Figure 4 Scatter plots of MODIS-Aqua chl-a match-ups at a maximum time difference of ΔT=±24 h. OWT is indicated by colour. Dashed line is 1:1, solid line is regression for all water types combined. Error bars represent the standard deviation within the match-up area.

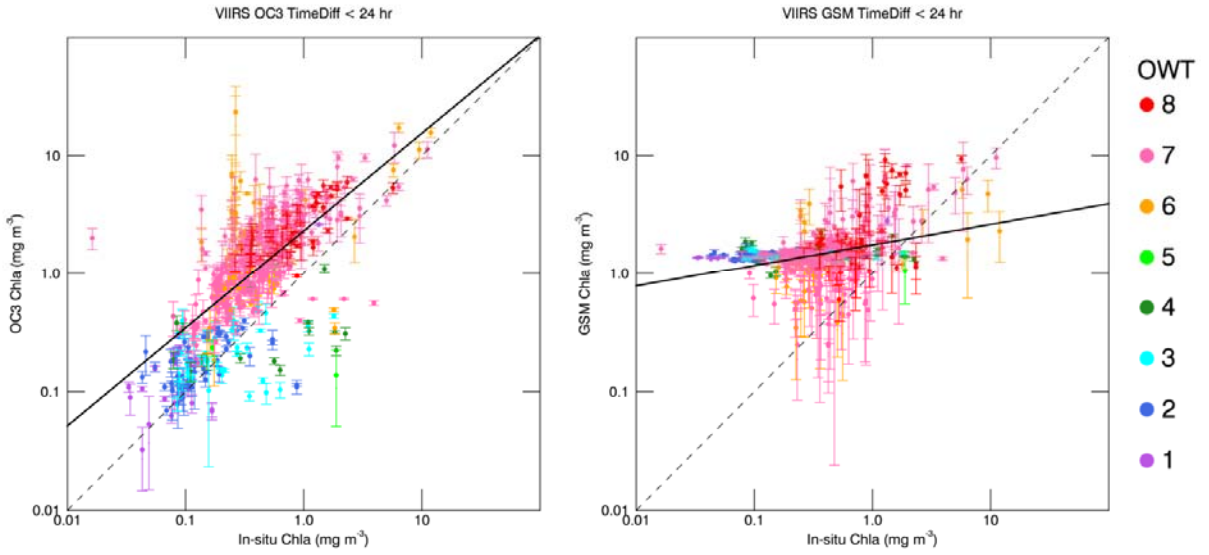

Figure 5 Scatter plots of VIIRS chl-a match-ups at a maximum time difference of ΔT=±24 h. OWT is indicated by colour. Dashed line is 1:1, solid line is regression for all water types combined. Error bars represent the standard deviation within the match-up area.

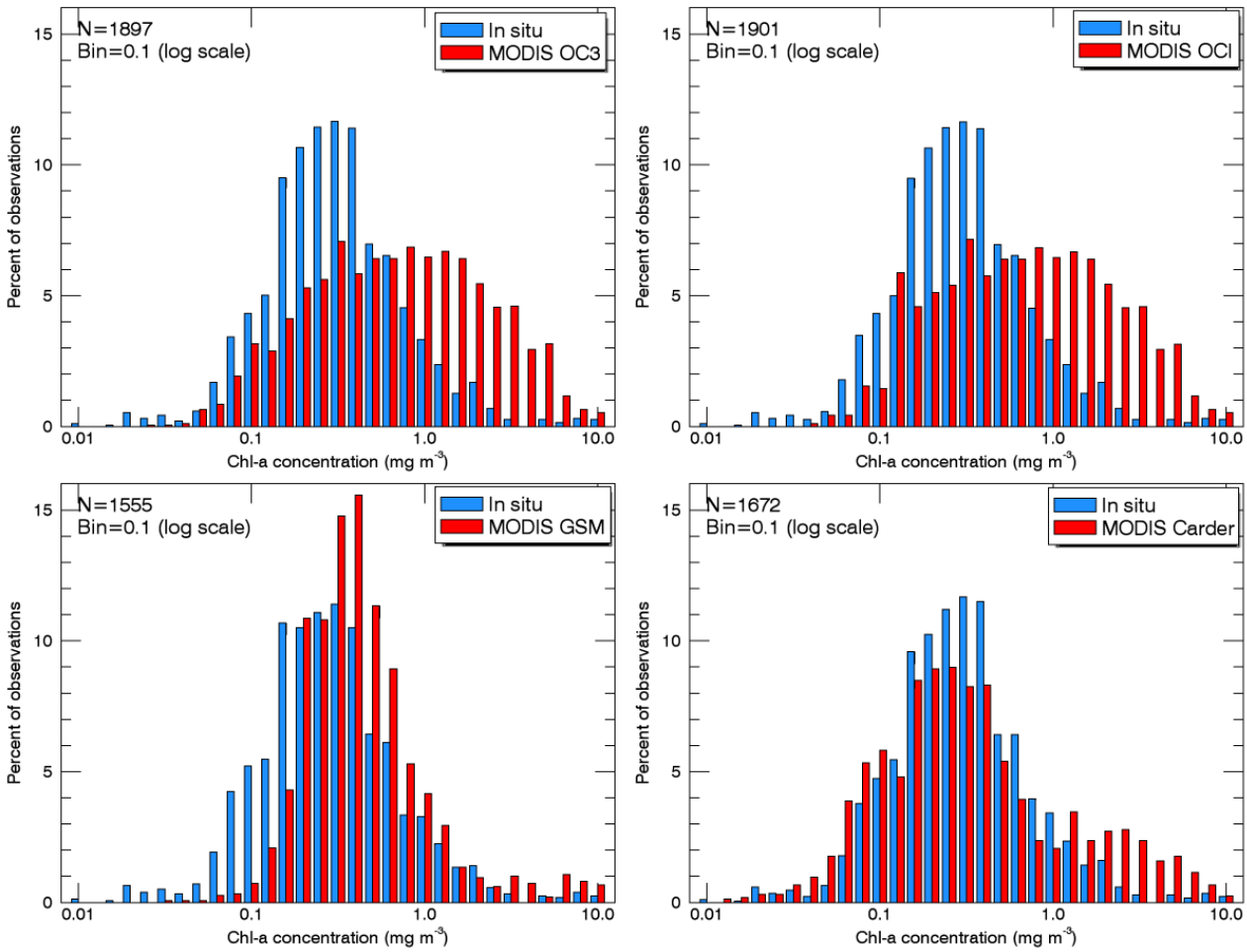

Figure 6 Histograms of chl-a derived from *in situ* and MODIS Aqua data. Note histogram bins are equal in log-transformed chl-a concentration.

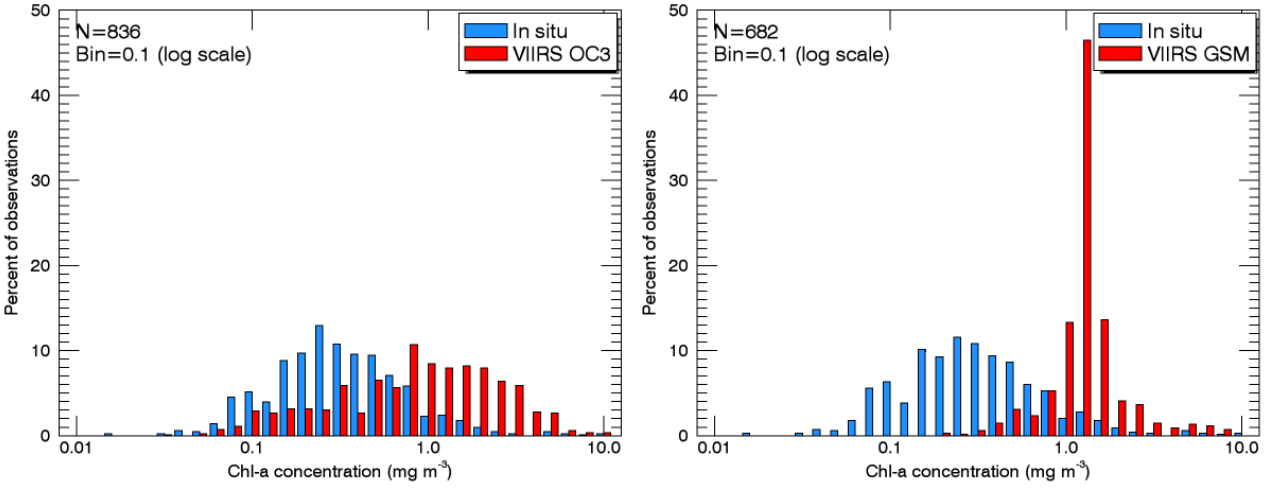

Figure 7 Histograms of chl-a derived from *in situ* and VIIRS data. Note histogram bins are equal in log-transformed chl-a concentration.

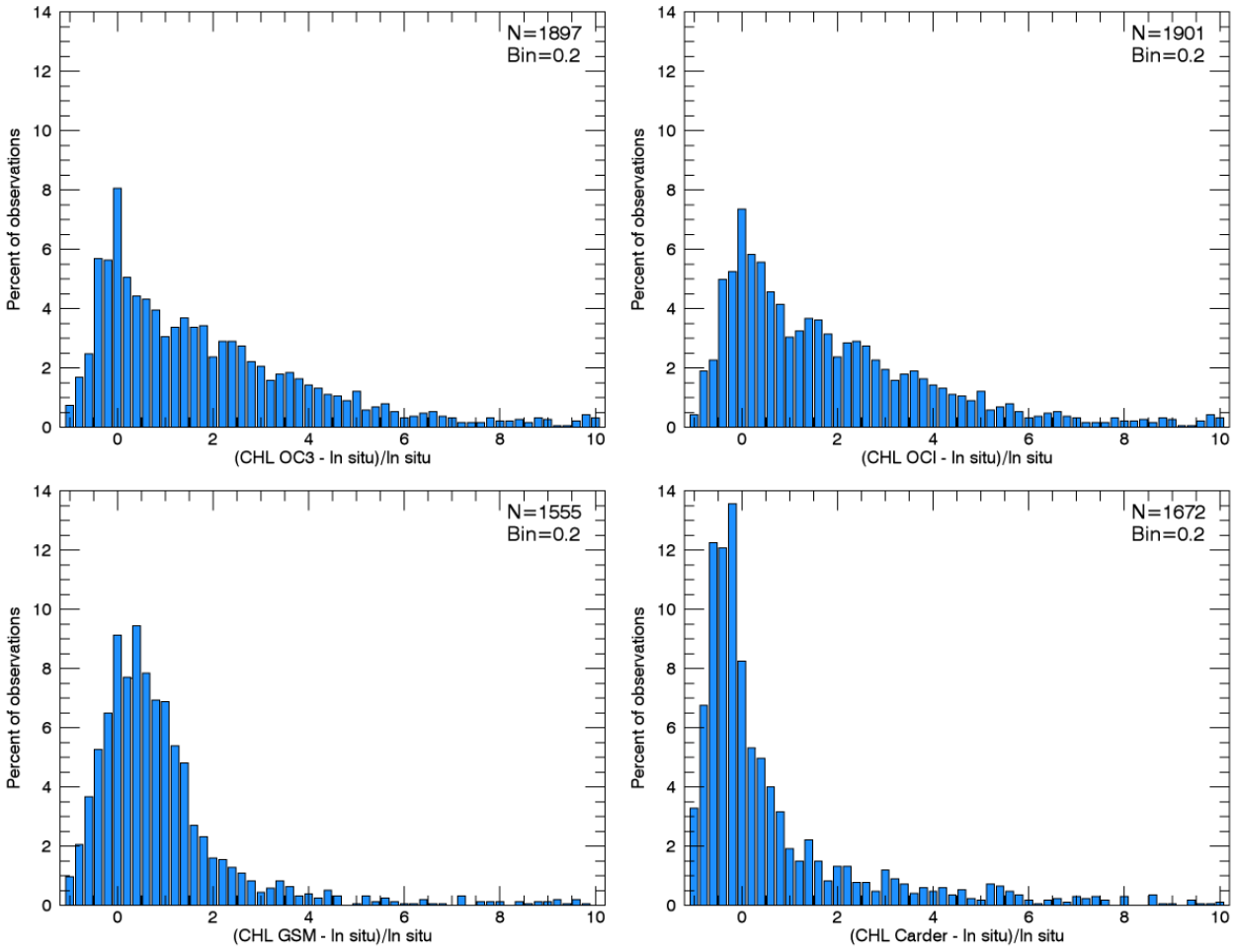

Figure 8 Histograms of the normalised difference chl-a concentration for MODIS Aqua.

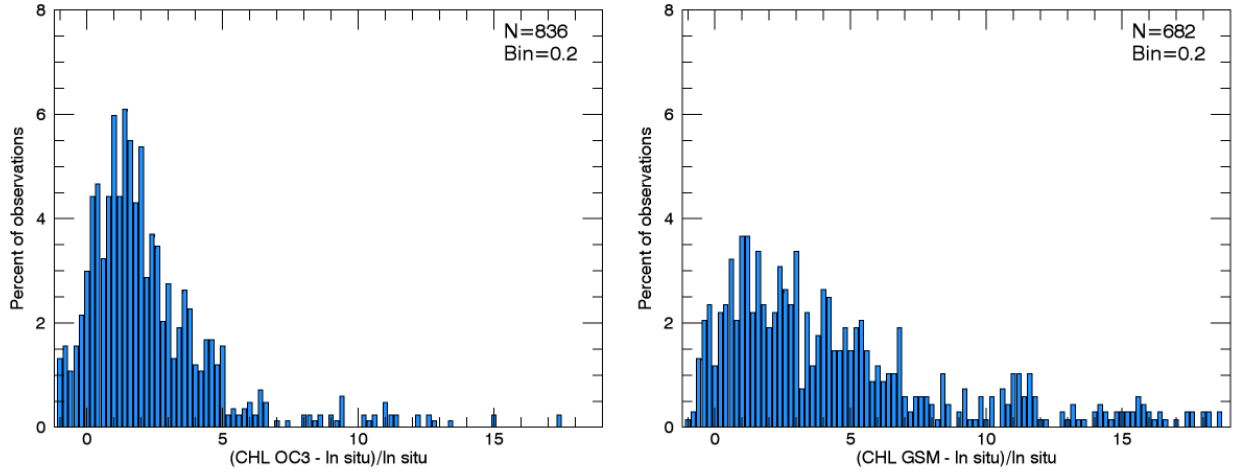

Figure 9 Histograms of the normalised difference chl-a concentration for VIIRS.

Table 1 Chl-a match-up statistics for the MODIS OC3 algorithm arranged by Optical Water Type at a maximum time difference of ±24 hours. Correlations marked with ** are statistically significant at the P<0.01 probability while those marked with * are statistically significant at P<0.05.

MODIS-Aqua OC3 ΔT=±24 h								
OWT	**1**	**2**	**3**	**4**	**5**	**6**	**7**	**8**
N	75	186	296	66	4	149	1048	73
R^2	0.2462**	0.3342**	0.0659**	0.2502**	0.1392	0.1908**	0.4118**	0.4984**
RMSE	0.3375	0.2308	0.3606	0.6067	0.9136	0.7514	0.6068	0.5021
10^{RMSE}	2.18	1.70	2.29	4.04	8.20	5.64	4.04	3.18
MAPE	80.94	45.04	109.15	366.32	470.76	756.45	328.43	216.73
Bias	0.0639	0.0501	0.0275	0.2486	0.3517	0.5938	0.5231	0.4627

Table 2 Same as table 1 but for the MODIS OCI algorithm.

MODIS-Aqua OCI ΔT=±24 h								
OWT	**1**	**2**	**3**	**4**	**5**	**6**	**7**	**8**
N	77	186	297	66	4	149	1048	73
R^2	0.2520**	0.2995**	0.0915**	0.2502**	0.1392	0.1908**	0.4118**	0.4984**
RMSE	0.3240	0.2383	0.3258	0.6067	0.9136	0.7514	0.6068	0.5021
10^{RMSE}	2.11	1.73	2.12	4.04	8.20	5.64	4.04	3.18
MAPE	70.56	51.52	110.14	366.32	470.76	756.45	328.44	216.73
Bias	0.0533	0.0831	0.0555	0.2486	0.3517	0.5938	0.5231	0.4627

Table 3 Same as table 1 but for the MODIS GSM algorithm.

MODIS-Aqua GSM ΔT=±24 h								
OWT	**1**	**2**	**3**	**4**	**5**	**6**	**7**	**8**
N	76	187	300	67	5	66	786	67
R^2	0.2121**	0.3331**	0.0727**	0.0461	0.6735	0.5326**	0.4363**	0.1993**
RMSE	0.4120	0.3305	0.3843	0.6859	0.6954	0.5704	0.5006	0.3874
10^{RMSE}	2.58	2.14	2.42	4.85	4.96	3.72	3.17	2.44
MAPE	157.13	103.04	189.71	527.17	270.91	309.98	272.34	146.94
Bias	0.2735	0.2494	0.1991	0.3218	0.3931	0.3219	0.2784	0.2841

Table 4 Same as table 1 but for the MODIS Carder algorithm.

MODIS-Aqua Carder ΔT=±24 h								
OWT	**1**	**2**	**3**	**4**	**5**	**6**	**7**	**8**
N	76	184	294	65	4	111	870	68
R^2	0.2267**	0.3374**	0.0603**	0.1260**	0.2274	0.2654**	0.2935**	0.0795*
RMSE	0.4174	0.2559	0.4089	0.5750	0.7723	0.6082	0.4838	0.3587
10^{RMSE}	2.61	1.80	2.56	3.76	5.92	4.06	3.05	2.28
MAPE	54.88	34.85	101.72	276.76	283.40	398.19	184.48	115.90
Bias	-0.1156	-0.1104	-0.1166	0.0959	0.1894	0.3687	0.1570	0.1597

Table 5 Chl-a match-up statistics for the MODIS OC3 algorithm arranged by Optical Water Type at a maximum time difference of ±2 hours. Correlations marked with ** are statistically significant at the P<0.01 probability while those marked with * are statistically significant at P<0.05.

MODIS-Aqua OC3 ΔT=±2 h								
OWT	**1**	**2**	**3**	**4**	**5**	**6**	**7**	**8**
N	38	112	171	33	2	84	600	45
R^2	0.3858**	0.4100**	0.0996**	0.1493*	-	0.2690**	0.3727**	0.4620**
RMSE	0.3559	0.2255	0.3593	0.7291	-	0.7218	0.5995	0.5129
10^{RMSE}	2.27	1.68	2.29	5.36	-	5.27	3.98	3.26
MAPE	96.58	39.80	96.61	513.78	-	590.86	325.21	223.41
Bias	0.1159	0.0245	0.0087	0.4129	-	0.5645	0.5049	0.4644

Table 6 Same as table 5 but for the MODIS OCI algorithm.

MODIS-Aqua OCI ΔT=±2 h								
OWT	**1**	**2**	**3**	**4**	**5**	**6**	**7**	**8**
N	38	112	171	33	2	84	600	45
R^2	0.3455**	0.3829**	0.1486**	0.1493*	-	0.2690**	0.3727**	0.4620**
RMSE	0.3536	0.2315	0.3053	0.7291	-	0.7218	0.5995	0.5129
10^{RMSE}	2.26	1.70	2.02	5.36	-	5.27	3.98	3.26
MAPE	86.05	46.23	97.16	513.78	-	590.86	325.21	223.41
Bias	0.1034	0.0521	0.0443	0.4129	-	0.5645	0.5049	0.4644

Table 7 Same as table 5 but for the MODIS GSM algorithm.

MODIS-Aqua GSM ΔT=±2 h								
OWT	**1**	**2**	**3**	**4**	**5**	**6**	**7**	**8**
N	37	112	173	33	3	31	452	42
R^2	0.3113**	0.3739**	0.1321**	0.0156	0.9654	0.7198**	0.3793**	0.1430*
RMSE	0.4741	0.3277	0.3574	0.8351	0.6283	0.5220	0.4949	0.4277
10^{RMSE}	2.98	2.13	2.28	6.84	4.25	3.33	3.13	2.68
MAPE	205.94	100.31	164.47	807.55	126.84	212.15	255.63	174.93
Bias	0.3111	0.2297	0.1765	0.5206	0.3312	0.2831	0.2644	0.2953

Table 8 Same as table 5 but for the MODIS Carder algorithm.

MODIS-Aqua Carder ΔT=±2 h								
OWT	**1**	**2**	**3**	**4**	**5**	**6**	**7**	**8**
N	37	111	168	33	2	63	498	42
R^2	0.5185**	0.2988**	0.0941**	0.0815	-	0.1875**	0.2357**	0.0717
RMSE	0.3035	0.2867	0.3959	0.6816	-	0.6655	0.4920	0.3955
10^{RMSE}	2.01	1.94	2.49	4.80	-	4.63	3.10	2.49
MAPE	53.42	38.49	91.06	443.62	-	518.44	186.42	140.67
Bias	-0.0115	-0.1364	-0.1442	0.2782	-	0.3812	0.1249	0.1934

Table 9 Chl-a match-up statistics for the MODIS OC3 algorithm arranged by time difference. Correlations marked with ** are statistically significant at the P<0.01 probability while those marked with * are statistically significant at P<0.05.

MODIS-Aqua OC3					
Time difference	**±24 h**	**±12 h**	**±6 h**	**±3 h**	**±2 h**
N	1897	1247	1187	1133	1085
R^2	0.4525**	0.4470**	0.4577**	0.4603**	0.4542**
RMSE	0.5473	0.5307	0.5359	0.5395	0.5414
10^{RMSE}	3.526	3.394	3.435	3.464	3.478
MAPE	287.58	261.45	267.30	271.44	273.23
Bias	0.3746	0.3460	0.3567	0.3629	0.3628

Table 10 Same as table 9 but for the MODIS OCI algorithm.

MODIS-Aqua OCI					
Time difference	**±24 h**	**±12 h**	**±6 h**	**±3 h**	**±2 h**
N	1901	1251	1191	1134	1086
R^2	0.4594**	0.4573**	0.4679**	0.4662**	0.4595**
RMSE	0.5435	0.5249	0.5304	0.5345	0.5362
10^{RMSE}	3.495	3.349	3.391	3.424	3.437
MAPE	287.50	261.11	266.80	271.63	273.45
Bias	0.3811	0.3527	0.3628	0.3703	0.3705

Table 11 Same as table 9 but for the MODIS GSM algorithm.

MODIS-Aqua GSM					
Time difference	**±24 h**	**±12 h**	**±6 h**	**±3 h**	**±2 h**
N	1555	1042	982	928	883
R^2	0.4318**	0.4076**	0.4191**	0.4187**	0.4086**
RMSE	0.4652	0.4660	0.4678	0.4675	0.4632
10^{RMSE}	2.919	2.924	2.936	2.934	2.905
MAPE	237.52	237.67	237.41	237.22	230.81
Bias	0.2638	0.2555	0.2570	0.2601	0.2567

Table 12 Same as table 9 but for the MODIS Carder algorithm.

MODIS-Aqua Carder					
Time difference	**±24 h**	**±12 h**	**±6 h**	**±3 h**	**±2 h**
N	1672	1115	1053	997	954
R^2	0.4034**	0.3811**	0.3886**	0.3791**	0.3658**
RMSE	0.4562	0.4560	0.4588	0.4617	0.4651
10^{RMSE}	2.859	2.857	2.876	2.895	2.918
MAPE	162.79	165.39	170.59	173.86	175.72
Bias	0.0789	0.0640	0.0701	0.0721	0.0666

Table 13: Chl-a match-up statistics for the VIIRS OC3 algorithm arranged by Optical Water Type at a maximum time difference of ±24 hours. Correlations marked with ** are statistically significant at the P<0.01 probability while those marked with * are statistically significant at P<0.05.

VIIRS OC3 ΔT=±24 h								
OWT	**1**	**2**	**3**	**4**	**5**	**6**	**7**	**8**
N	31	66	45	17	4	115	479	79
R^2	0.5300**	0.0692*	0.1226*	0.0801	0.1072	0.1024**	0.4409**	0.5090**
RMSE	0.3392	0.3369	0.3352	0.5481	0.9902	0.8108	0.5815	0.5278
10^{RMSE}	2.18	2.17	2.16	3.53	9.78	6.47	3.82	3.37
MAPE	96.00	70.11	61.48	98.14	172.73	799.43	331.93	233.99
Bias	0.1729	0.1023	-0.0017	-0.1404	0.0093	0.6658	0.5129	0.4885

Table 14 Same as table 13 but for the VIIRS GSM algorithm.

VIIRS GSM ΔT=±24 h								
OWT	**1**	**2**	**3**	**4**	**5**	**6**	**7**	**8**
N	31	66	45	17	3	66	375	79
R^2	0.6613**	0.0364	0.0019	0.0076	0.9973*	0.1213**	0.1187**	0.2149**
RMSE	1.2336	1.0558	0.9301	0.7938	0.9797	0.6620	0.6655	0.5386
10^{RMSE}	17.12	11.37	8.51	6.22	9.54	4.59	4.63	3.46
MAPE	1619.23	1100.60	787.02	569.39	263.65	368.38	420.69	244.43
Bias	1.1572	0.9960	0.8473	0.5506	0.3542	0.5242	0.5760	0.4562

Table 15 Chl-a match-up statistics for the VIIRS OC3 algorithm arranged by Optical Water Type at a maximum time difference of ±2 hours. Correlations marked with ** are statistically significant at the P<0.01 probability while those marked with * are statistically significant at P<0.05.

VIIRS OC3 ΔT=±2 h								
OWT	**1**	**2**	**3**	**4**	**5**	**6**	**7**	**8**
N	9	40	29	8	1	75	307	41
R^2	0.4159	0.0122	0.0820	0.0749	-	0.3045**	0.3859**	0.5340**
RMSE	0.3846	0.3900	0.3657	0.6939	-	0.7057	0.5855	0.5020
10^{RMSE}	2.42	2.45	2.32	4.94	-	5.08	3.85	3.18
MAPE	112.15	74.56	70.96	82.90	-	443.55	352.88	208.85
Bias	0.2856	0.0581	0.0199	-0.3366	-	0.6048	0.5058	0.4572

Table 16 Same as table 15 but for the VIIRS GSM algorithm.

VIIRS GSM ΔT=±2 h								
OWT	**1**	**2**	**3**	**4**	**5**	**6**	**7**	**8**
N	9	40	29	8	1	47	241	41
R^2	0.0258	0.0167	0.0006	0.0086	-	0.0978*	0.0810**	0.1541*
RMSE	1.4559	1.0654	0.9179	0.7218	-	0.6739	0.6694	0.5235
10^{RMSE}	28.57	11.63	8.28	5.27	-	4.72	4.67	3.34
MAPE	1911.14	1127.40	750.42	397.78	-	376.48	441.17	224.67
Bias	1.2758	0.9795	0.8165	0.3579	-	0.4995	0.5673	0.4202

Table 17 Chl-a match-up statistics for the VIIRS OC3 algorithm arranged by time difference. Correlations marked with ** are statistically significant at the P<0.01 probability while those marked with * are statistically significant at P<0.05.

VIIRS OC3					
Time difference	**±24 h**	**±12 h**	**±6 h**	**±3 h**	**±2 h**
N	836	566	552	529	510
R^2	0.4230**	0.4117**	0.4089**	0.4032**	0.3978**
RMSE	0.5783	0.5602	0.5646	0.5666	0.5684
10^{RMSE}	3.787	3.633	3.670	3.686	3.702
MAPE	337.49	295.76	301.56	304.90	307.77
Bias	0.4432	0.4209	0.4316	0.4362	0.4362

Table 18 Chl-a match-up statistics for the VIIRS GSM algorithm arranged by time difference. Correlations marked with ** are statistically significant at the P<0.01 probability while those marked with * are statistically significant at P<0.05.

VIIRS GSM					
Time difference	**±24 h**	**±12 h**	**±6 h**	**±3 h**	**±2 h**
N	682	464	451	432	416
R^2	0.1089**	0.0728**	0.0735**	0.0784**	0.0734**
RMSE	0.7463	0.7435	0.7368	0.7338	0.7329
10^{RMSE}	5.575	5.540	5.456	5.417	5.406
MAPE	542.67	545.17	535.89	530.94	530.55
Bias	0.6405	0.6268	0.6195	0.6166	0.6133

Acknowledgments

We kindly acknowledge the MODIS and VIIRS Characterisation Support Teams and associated NASA and NOAA personnel for their in-orbit sensor calibration efforts.

We also thank the Ocean Biological Processing Group at NASA GSFC, the SeaDAS Development Group at NASA GSFC and Brockmann Consult GmbH for the distribution and maintenance of the SeaDAS software package.

We are grateful to our colleagues Dr David Blondeau-Patissier and Dr Timothy Malthus who helped reviewing this report and acknowledge Paige Kelly for her work on the IMOS Bio-optical Data Base.

All data contributors to the IMOS Bio-optical Data Base are duly acknowledged, explicitly the Australian Institute of Marine Science, James Cook University and the CSIRO.

This research activity was undertaken with the assistance of resources and services from the National Computational Infrastructure (NCI), which is supported by the Australian Government.

Appendix A Statistics

The statistical measures used in this report are described by the following equations. In the case of MAPE, *x* is the *in situ* measurement and *y* is the satellite observation and *N* is the number of samples (valid match-ups).

$$MAPE = \frac{100}{N}\sum\frac{|y-x|}{x}$$

For calculation of Bias, RMSE and linear correlation coefficient the input data are log transformed, such that *x* is the $\log_{10}$ of the *in situ* measurement and *y* is the $\log_{10}$ of the satellite observation and *N* is the number of samples (valid match-ups).

$$Bias = \frac{1}{N}\sum(y-x)$$

$$RMSE = \sqrt{\frac{1}{N}(x-y)^2}$$

$$R^2 = \left[\frac{\sum xy - \frac{(\sum x)(\sum y)}{N}}{\sqrt{\left(\sum x^2 - \frac{(\sum x)^2}{N}\right)\left(\sum y^2 - \frac{(\sum y)^2}{N}\right)}}\right]^2$$

Appendix B Data Repositories

The AODN data portal (https://portal.aodn.org.au) is the primary means of discovering and accessing all IMOS satellite data products. The portal allows browsing of the gridded (mapped) products, download of spatio-temporal subsets in netCDF, and access via THREDDS, which supports OPeNDAP.

A copy of all gridded data sets is also held by CSIRO where a THREDDS server supports direct file access, and also the OPeNDAP and OGC Web mapping service protocols (http://rs-data1-mel.csiro.au/imos-srs). An experimental ERDDAP server (created by NOAA in the US) is also available to access selected gridded data products (http://rs-data2-mel.csiro.au/erddap/index.html).

For users requiring direct access to any of the MODIS or VIIRS data sets including the unmapped data in swath format, all data are openly available on the large data storage at the NCI in Canberra, from where they are exposed in the file-system and via WWW and THREDDS servers.

(http://dap.nci.org.au/thredds/remoteCatalogService?catalog=http://dapds00.nci.org.au/thredds/catalog/u39/public/data/catalog.xml)

The IMOS Bio-optical Data Base is available through the AODN portal.

References

Carder K. L., Chen F. R., Lee Z. P., Hawes S. K. and Cannizzaro J. P. (2003), MODIS Ocean Science Team Algorithm Theoretical Basis Document, ATBD 19, Case 2 Chlorophyll a, Version 7, URL: http://modis.gsfc.nasa.gov/data/atbd/atbd_mod19.pdf (accessed 28 August 2014).

Carder K. L., Chen F. R., Lee Z. P., Hawes S. K. and Kamykowski D. (1999), Semianalytic Moderate-Resolution Imaging Spectrometer algorithms for chlorophyll a and absorption with bio-optical domains based on nitrate-depletion temperatures, *Journal of Geophysical Research*: Oceans, 104(C3), 5403-5421.

Fu G., Baith K. S., and McClain C. R. (1998), SeaDAS: The SeaWiFS Data Analysis System, in *Proceedings of the 4th Pacific Ocean Remote Sensing Conference*, Qingdao, China.

Hu C., Lee Z., & Franz B. A. (2012), Chlorophyll-a algorithms for oligotrophic oceans: A novel approach based on three-band reflectance difference. *Journal of Geophysical Research*, 117.

Maritorena S., Siegel D. A., and Peterson A. R. (2002), Optimization of a semianalytical ocean color model for global-scale applications, *Applied Optics*, 41(15), 2705-2714.

Moore T. S., Campbell J. W. and Dowell M. D. (2009), A class-based approach to characterizing and mapping the uncertainty of the MODIS ocean chlorophyll product, *Remote Sensing of Environment,* 113(11), 2424-2430.

O'Reilly J. E., Maritorena S., Siegel D., O'Brien M. O., Toole D., Mitchell B. G., Kahru M., Chavez F. P., Strutton P., Cota G. F., Hooker S. B., McClain C. R., Carder K. L., Muller-Karger F., Harding L., Magnuson A., Phinney D., Moore G. F., Aiken J., Arrigo K. R., Letelier R. M., Culver M. (2000), Ocean Color Chlorophyll a Algorithms for SeaWiFS, OC2, and OC4: Version 4, In SeaWiFS Postlaunch Calibration and Validation Analyses, Volume 11, Part 3, (McClain C. R., Ed.), pages 9-23, Greenbelt, Md.: Goddard Space Flight Center.

Schroeder T., Lovell J., King K., Clementson L. and Scott R., (2016), IMOS Ocean Colour Validation Report 2015-16, Report to the Integrated Marine Observing System (IMOS), CSIRO Oceans and Atmosphere, 33 pp.

Wang, M. and Son S. (2016), VIIRS-derived chlorophyll-a using the ocean color index method, *Remote Sensing of Environment,* 182, 141-149.